Published in final edited form as:

Clin Cancer Res. 2017 November 01; 23(21): 6629–6639. doi:10.1158/1078-0432.CCR-17-0668.

p53 Nongenotoxic Activation and mTORC1 Inhibition Lead to Effective Combination for Neuroblastoma Therapy

Myrthala Moreno-Smith[1], **Anna Lakoma**[2], **Zaowen Chen**[1], **Ling Tao**[1], **Kathleen A. Scorsone**[1], **Linda Schild**[3], **Kevin Aviles-Padilla**[4], **Rana Nikzad**[4], **Yankai Zhang**[1], **Rikhia Chakraborty**[1], **Jan J. Molenaar**[3], **Sanjeev A. Vasudevan**[2], **Vivien Sheehan**[1], **Eugene S. Kim**[2], **Silke Paust**[4], **Jason M. Shohet**[1], and **Eveline Barbieri**[1]

[1]Department of Pediatrics, Section of Hematology-Oncology, Texas Children's Cancer and Hematology Centers, Baylor College of Medicine, Houston, Texas [2]Division of Pediatric Surgery, Michael E. DeBakey Department of Surgery, Baylor College of Medicine, Houston, Texas [3]Department of Oncogenomics, Academic Medical Center, University of Amsterdam, Amsterdam, the Netherlands [4]Department of Pediatrics, Center for Human Immunobiology, Texas Children's Hospital, Baylor College of Medicine, Houston, Texas

Abstract

Purpose—mTORC1 inhibitors are promising agents for neuroblastoma therapy; however, they have shown limited clinical activity as monotherapy, thus rational drug combinations need to be explored to improve efficacy. Importantly, neuroblastoma maintains both an active p53 and an aberrant mTOR signaling.

Experimental Design—Using an orthotopic xenograft model and modulating p53 levels, we investigated the antitumor effects of the mTORC1 inhibitor temsirolimus in neuroblastoma expressing normal, decreased, or mutant p53, both as single agent and in combination with first- and second-generation MDM2 inhibitors to reactivate p53.

Corresponding Author: E. Barbieri, Baylor College of Medicine, Feigin 750.01, 1102 Bates, Houston, TX 77030. Phone: 832-824-4747; exbarbie@txch.org.

Note: Supplementary data for this article are available at Clinical Cancer Research Online (http://clincancerres.aacrjournals.org/).

Disclaimer: The manuscript contains only original material, which has not been published and is not under consideration for publication elsewhere. No author has any affiliation or financial involvement with any entity with a financial interest in the work presented here.

Disclosure of Potential Conflicts of Interest

No potential conflicts of interest were disclosed.

Authors' Contributions

Conception and design: M. Moreno-Smith, Z. Chen, E.S. Kim, S. Paust, J.M. Shohet, E. Barbieri

Development of methodology: Z. Chen, R. Chakraborty, V. Sheehan, E.S. Kim, J.M. Shohet, E. Barbieri

Acquisition of data (provided animals, acquired and managed patients, provided facilities, etc.): M. Moreno-Smith, A. Lakoma, Z. Chen, L. Tao, K.A. Scorsone, L. Schild, K. Aviles-Padilla, R. Nikzad, Y. Zhang, R. Chakraborty, J.J. Molenaar, S.A. Vasudevan, V. Sheehan, E.S. Kim, S. Paust, E. Barbieri

Analysis and interpretation of data (e.g., statistical analysis, biostatistics, computational analysis): M. Moreno-Smith, A. Lakoma, Z. Chen, L. Tao, K. Aviles-Padilla, R. Nikzad, S. Paust, E. Barbieri

Writing, review, and/or revision of the manuscript: M. Moreno-Smith, A. Lakoma, L. Tao, E.S. Kim, J.M. Shohet, E. Barbieri

Administrative, technical, or material support (i.e., reporting or organizing data, constructing databases): Z. Chen

Study supervision: S.A. Vasudevan, E. Barbieri

Results—Nongenotoxic p53 activation suppresses mTOR activity. Moreover, p53 reactivation via RG7388, a second-generation MDM2 inhibitor, strongly enhances the *in vivo* antitumor activity of temsirolimus. Single-agent temsirolimus does not elicit apoptosis, and tumors rapidly regrow after treatment suspension. In contrast, our combination therapy triggers a potent apoptotic response in wild-type p53 xenografts and efficiently blocks tumor regrowth after treatment completion. We also found that this combination uniquely led to p53-dependent suppression of survivin whose ectopic expression is sufficient to rescue the apoptosis induced by our combination.

Conclusions—Our study supports a novel highly effective strategy that combines RG7388 and temsirolimus in wild-type p53 neuroblastoma, which warrants testing in early-phase clinical trials.

Introduction

Neuroblastoma is a MYCN-driven neural crest malignancy that accounts for approximately 15% of all pediatric cancer mortality (1). At diagnosis, neuroblastoma has wild-type p53 and intact apoptosis response. However, at relapse, about 35% of patients accrue upstream defects in p53 regulation (2). MYCN serves multiple roles in neuroblastoma, such as altering metabolic programs, supporting angiogenesis, and inhibiting differentiation (3–5). The MYC genes *(c-Myc, N-myc, and L-myc)* drive tumorigenesis in part by activation of the mTOR pathway, a master regulator of translation, and protein synthesis (6, 7). Thus, effective inhibition of mTOR functions represents a potential strategy for therapeutic targeting of MYC in neuroblastoma and other cancers.

The mTOR pathway is a major integrator of cell metabolic responses to growth factors and nutrients, regulating cellular survival, including transcription and translation, cell motility, and angiogenesis (8). The PI3K/mTOR signaling pathway is constitutively active in neuroblastoma tumors and deregulates cell metabolism via increased expression of multiple growth factor receptors, including insulin-like growth factor I receptor (IGFR), epidermal growth factor receptor (EGFR), tyrosine receptor kinase B (TrkB), and platelet-derived growth factor receptor B (PDGF; refs. 9–11). Importantly, high PI3K/mTOR activity and phosphorylated AKT correlate with drug resistance and poor prognosis (12). Moreover, the PI3K/AKT/mTOR pathway drives oncogenic stabilization of MYCN protein (13). This is supported by findings that small-molecule inhibitors of PI3K/mTOR are effective in preclinical neuroblastoma models through MYCN destabilization (14, 15), and by transcriptome analyses of MYCN-amplified neuroblastoma tumors confirming tumor-specific activation of mTOR signaling (16).

Temsirolimus is a potent and selective inhibitor of mTOR complex 1 (mTORC1) with on-target activity at low concentrations (17). In early phase clinical trials, temsirolimus was well-tolerated and demonstrated some degree of efficacy in children with solid tumors (18). However, phase II studies demonstrated limited activity of temsirolimus as monotherapy (19). Furthermore, resistance to temsirolimus through increased AKT phosphorylation has also been described (20). This prompted to combine temsirolimus with chemotherapeutic agents such as irinotecan, temozolomide (21), and vinblastine (22).

Neuroblastoma tumors maintain the two opposing pathways of active p53 that mediates growth arrest and apoptosis, and aberrant mTOR signaling that mediates growth and proliferation. Recent findings clearly demonstrate a molecular mechanism linking p53 function with mTOR repression. In response to stress, p53 transcribes a group of negative regulators of the IGF/AKT/mTOR pathway, including IGF-BP3, PTEN, TSC2, AMPK β1, and SESN 1 and 2, all of which suppress mTOR signaling (23, 24) and initiate cell-cycle arrest, DNA repair, senescence, or apoptosis depending on tumor type and degree of stress (25). In addition, p53-mediated induction of autophagy occurs through mTOR inhibition (26). Supporting the link between p53 and mTOR, SESN2-deficient mice fail to inhibit mTOR signaling upon genotoxic challenge (27). Based on these findings linking p53 activation to mTOR suppression, we hypothesized that p53 activation via MDM2 inhibition would sensitize neuroblastoma tumors to mTORC1 inhibitors.

We and others have previously shown that the first-generation MDM2 inhibitor Nutlin 3a stabilizes p53, induces the expression of p53 target genes, and sensitizes neuroblastoma cells to conventional chemotherapy (28–30). Recently, second-generation inhibitors of the p53–MDM2 interaction with superior potency and selectivity (such as RG7388) have been developed. RG7388 showed promising preclinical efficacy against osteosarcoma and neuroblastoma, and clinical responses in completed phase I clinical trials (NCT01773408; refs. 31–33).

We present here a highly effective *in vivo* combination therapy by simultaneous nongenotoxic p53 activation (via RG7388) and mTORC1 inhibition (via temsirolimus). We demonstrate profound inhibition of *in vivo* tumor growth following the combination therapy in both MYCN-amplified and nonamplified tumor models. We also demonstrate markedly increased apoptosis and lack of tumor regrowth following the dual treatment. Overall, we provide strong preclinical data and a model supporting future clinical development of this therapeutic strategy.

Materials and Methods

Cell culture, antibodies, and expression vectors

Reagents, cell culture, and antibodies are described in Supplementary Experimental Procedures. For p53 shRNA, second-generation lentiviruses expressing shp53 and shLuc control were used as described in ref. (29). Briefly, 293T cells were transfected with pLSLPw construct along with packaging plasmids, pVSVG, and pLV-CMV-delta 8.2 by using lipofectamine 2000. Virus-containing supernatants were collected at 48 and 72 hours and cells transduced in the presence of 8 mg/mL polybrene (Sigma). For survivin overexpression, expression constructs were produced from a PCR product of survivin (CCDS11755.1: isoform 1) obtained from IMR32 cDNA and cloned into pLenti4/TO/V5-Dest according to the manufacturer's procedures (Invitrogen).

Cell proliferation and apoptosis

For cell proliferation, 3-(4,5-Dimethylthiazol-2-yl)-2,5-diphenyltetrazolium bromide (MTT) assays were performed as in ref. (30). To measure cell size, LAN5 Si CTRL or LAN5 Si p53

cells were imaged under Olympus Microscope IX71 with ×20 magnification. Areas of 500 to 1,000 cells per group were analyzed using Image J. Average area per cell was plotted as an indication of cell size. For apoptosis determination, Terminal Deoxynucleotidyl Transferase assay was performed following protocol as in ref. (30). Apoptosis was measured by FACS analysis of the percentage of cells positive for avidin FITC 48 hours after treatment. Error bars are SD ($n = 3$). Caspase 3 and 7 activation was also measured using a Caspase-Glo assay kit (Promega). Briefly, cells were seeded in 96-well plate at 5,000 cells/well and then subjected to different treatments for 24 to 48 hours. Equal volume of caspase reagent was added to the wells and luminescence was measured in plate-reading luminometer after 3 hours. Error bars are SD ($n = 3$).

RNA isolation and real-time qPCR

Real-time qPCR assays were carried out as described in Supplementary Experimental Procedures.

In vivo models

In vivo studies were approved by the Institutional Animal Care and Use Committee at Baylor College of Medicine (AN 4810). Orthotopic xenografts of human neuroblastoma were generated as described previously (34). An inoculum of 10^6 tumor cells in 0.1 mL of PBS was injected under the renal capsule of 4- to 6-week-old female athymic Ncr nude mice (Taconic). Two weeks after cell implantation and confirmation of successful tumor engraftment by bioluminescent imaging (Xenogen IVIS 100 System, Caliper Life Sciences), mice were randomized and divided into treatment groups. Tumor growth was monitored by bioluminescent imaging after cell implantation. Four to 7 weeks after implantation, mice were sacrificed, tumors were resected, weighed, and preserved in 4% paraformaldehyde for immunohistochemical analysis. All animal data were compared using Kruskal–Wallis and Mann–Whitney tests.

Peripheral blood mononuclear cell isolation and flow cytometry

Peripheral blood mononuclear cell (PBMC) isolation and analysis are described in Supplementary Experimental Procedures.

$CD34^+$ cell isolation and colony-forming unit assay

The effect of the combination therapy on maturation and differentiation of $hCD34^+$ hematopoietic stem-progenitor cell (HSPC) was evaluated by colony-forming unit (CFU) assay (35). $CD34^+$ cell isolation and CFU assay are described in Supplementary Experimental Procedures.

Generation and treatment of humanized NSG mice

A detailed description of the generation of humanized NSG mice is described in Supplementary Experimental Procedures. Briefly, NOD/SCID/IL2rγ^{null} pups were irradiated 24 hours after birth with a single dose of 110 cGy. Following irradiation, 0.75×10^5 $CD34^+$ HSCs were intrahepatically injected. Six weeks after injection, peripheral blood was collected and analyzed for human lymphocyte reconstitution by assessment of human

versus mouse $CD45^+$ cell presence. Mice with greater than 40% human $CD45^+$ reconstitution were selected (36).

Statistical analysis

All *in vitro* assays, including flow cytometry analyses, proliferation, and qPCR analyses, are expressed as mean ± SD and performed in triplicate. Data were compared using the Student *t* test. Tumor weights are expressed as mean ± SEM and compared using Kruskal–Wallis and Mann–Whitney tests; *P* values <0.05 were considered statistically significant.

Results

Functional p53 suppresses mTOR signaling in neuroblastoma cells and xenografts

mTORC1 is a critical mediator of cell growth and regulates cell size and protein synthesis through activation of its substrates, the ribosomal protein S6 kinase (p70S6K) and the eIF4E binding protein 1 (4EBP1). To confirm whether p53 regulates mTOR signaling in neuroblastoma, we silenced p53 expression in p53 wild-type lines via lentiviral-mediated siRNA (Supplementary Fig. S1) and used p70S6K phosphorylation as readout for mTOR activity. p70S6K activation can in turn be determined by phosphorylation of ribosomal S6 protein (pS6) at S235/236. As predicted, p53 knockdown cells showed a significant increase in cell size (Fig. 1A). Because mTOR signaling is a major regulator of cell size, we then looked at mTOR activity in cells expressing normal or decreased wild-type p53 levels. p53 knockdown cells showed a significant increase in pS6 levels, as determined by flow cytometry (Fig. 1B) and by Western blotting (Fig. 1C). They also have higher p4EBP1 levels (Fig. 1C), together indicating higher mTOR activity in these cells.

To evaluate the *in vivo* regulation of mTOR activity by p53, p53 wild-type and knockdown cells were then engrafted in nude mice using an orthotopic neuroblastoma model (34). Neuroblastoma tumors derived from p53 knockdown cells displayed low p53 levels compared with controls (Fig. 1D). They were also significantly larger ($P = 0.049$; Fig. 1E) and displayed a much higher mTOR activity measured as pS6 levels by immunohistochemistry (Fig. 1F), indicating that p53 efficiently suppresses mTOR signaling *in vivo*.

p53 induces the transcription of multiple upstream repressors of mTOR signaling. Evaluation of selected p53-dependent repressors in p53 wild-type and knockdown cells revealed that p53 activation is associated with increased expression levels of the mTOR signaling inhibitors sestrin 1 (SESN1), sestrin 2 (SESN2), tuberous sclerosis 2 (TSC2), and AMP-activated protein kinase β1 (AMPK β1). However, this upregulation was partially abrogated in the presence of reduced levels of p53, suggesting that p53 suppresses mTOR signaling via activation of these mTOR inhibitors (Fig. 2A).

To determine whether p53 activation suppresses mTOR signaling, we then treated neuroblastoma cells with a specific first-generation inhibitor of MDM2-p53 interaction (Nutlin 3a), which induces robust p53 stabilization (Supplementary Fig. S1). Treatment with Nutlin 3a resulted in a profound down-regulation of pS6 measured both by flow cytometry (Fig. 2B) and Western blotting (Fig. 2C). It also caused suppression of 4EBP1

phosphorylation as detected by Western blotting using p4EBP1 Thr37/46 and p4EBP1 Thr70 antibodies (Fig. 2C). Collectively, these data confirm that p53 activation effectively inhibits mTOR activity in neuroblastoma cells.

p53 silencing attenuates temsirolimus response *in vivo*

We first characterized the effect of temsirolimus on neuroblastoma tumor growth, confirming that the *in vivo* antitumor response of temsirolimus was indeed mediated by the inhibition of pS6 (Supplementary Fig. S2). To test whether p53 could affect the *in vivo* response to mTORC1 inhibition, we then determined the antitumor effects of temsirolimus in p53 wild-type (LAN5 Si CTRL), p53 knockdown (LAN5 Si p53), and p53 mutant (SK-N-AS) neuroblastoma orthotopic xenografts. Although mutant and silenced p53 enhanced neuroblastoma tumor growth (LAN5 Si p53 and SK-N-AS tumors were considerably larger than LAN5 Si CTRL tumors), p53 silencing significantly attenuated the *in vivo* antitumor effect of temsirolimus (Fig. 2D). A higher decrease in temsirolimus *in vivo* activity was observed in the p53-mutant xenografts (Fig. 2E), indicating that a functional p53 signaling enhances temsirolimus-mediated functions.

Nongenotoxic p53 activation strongly enhances *in vivo* antitumor activity of temsirolimus

Because most neuroblastoma tumors retain a functional p53 that once activated is able to efficiently suppress mTOR signaling (Fig. 2B), we then asked whether p53 activation via MDM2 inhibition could potentiate the antitumor activity of temsirolimus. Multiple p53 wild-type neuroblastoma cell lines (shown here LAN5 and CHLA255) were treated with increasing doses of Temsirolimus and fixed low doses of Nutlin 3a (first-generation MDM2 inhibitor) or RG7388 (second-generation MDM2 inhibitor), and cell viability and apoptosis were assessed. MDM2 inhibition enhances temsirolimus-mediated cell growth arrest in all p53 wild-type cell lines. However, no additional effect was detected in p53-mutant and p53-knockdown neuroblastoma cells (Supplementary Fig. S3A and S3B). Moreover, although single-agent temsirolimus and Nutlin 3a had a modest effect on apoptosis, the combination therapy led to a marked induction of apoptosis in both p53 wild-type SH-SY5Y and LAN5 cells (Supplementary Fig. S3C). This effect was again abrogated when the combination therapy was tested in p53-mutant cells (LAN1), confirming the dependency on a p53-dependent mechanism for apoptosis sensitization (Supplementary Fig. S3C, bottom right plot).

To then evaluate the *in vivo* activity and tolerability of our combination therapy, we used our orthotopic neuroblastoma model and RG7388, which has now completed phase I testing (31). Xenograft tumor models derived from LAN5 and SH-SY5Y neuroblastoma cell lines were generated. p53 wild-type MYCN-amplified luciferase-positive LAN5 cells were injected into the renal capsule of nude mice, and treatment was initiated 2 weeks after implantation. Vehicle control, temsirolimus (10 mg/kg), RG7388 (25 mg/kg), and the combination temsirolimus and RG7388 were given i.p. daily for 14 days, and effect on tumor growth was compared between groups at the end of the treatment. Temsirolimus exhibited potent antitumor effects as single agent ($P = 0.020$). However, the combination temsirolimus and RG7388 strongly potentiated the antitumor activity of both single monotherapies ($P = 0.043$ and $P = 0.010$, respectively; Fig. 3A). In addition, this drug

combination was very well tolerated, with all mice having normal body weight and parameters. To confirm our *in vivo* findings, a second p53 wild-type neuroblastoma line (SH-SY5Y) which differs in MYCN status, being MYCN nonamplified, was engrafted. Again, the combination of RG7388 and temsirolimus almost completely blocked the growth of these tumors (combination therapy vs. single-agent temsirolimus $P = 0.0087$, combination therapy vs. single-agent RG7388 $P = 0.013$; Fig. 3B), indicating that this combination is highly effective in our preclinical neuroblastoma models.

Nongenotoxic p53 activation prevents temsirolimus-mediated tumor regrowth after treatment suspension

Our *in vitro* data suggest that temsirolimus has mainly a cytostatic activity, being only modestly effective in inducing cell apoptosis (Supplementary Fig. S3C). Thus, we asked whether the *in vivo* response to temsirolimus as single agent or in combination with RG7388 was persistent after treatment withdrawal. For this study, we orthotopically engrafted the neuroblastoma line tested as most sensitive to temsirolimus *in vivo*, SH-SY5Y. We then divided the mice in three treatment groups of 20 mice each: vehicle control, temsirolimus (10 mg/kg), and temsirolimus and RG7388 (25 mg/kg). After 2 weeks of treatment, half of the mice were sacrificed and tumor weights assessed, and half of the mice were kept alive without any additional treatment for 3 weeks (Fig. 4A). Effects on tumor growth and apoptosis were examined in xenografts tumors after 2 weeks of treatment and after 3 weeks of treatment withdrawal. Temsirolimus treatment as single agent for 2 weeks resulted in a drastic inhibition of primary tumor growth. However, treatment withdrawal led to rapid and significant tumor regrowth, as documented by tumor weights (Fig. 4B) and bioluminescent imaging (Supplementary Fig. S4) at 3 weeks after treatment suspension. Notably, tumor regression was not associated with induction of apoptosis, supporting our *in vitro* data. In contrast, the combination of temsirolimus and RG7388 resulted in significant induction of apoptosis and prolongation of tumor control, which persisted 3 weeks after treatment completion ($P < 0.0001$; Fig. 4B), suggesting that p53-mediated apoptosis is required to maintain a stable *in vivo* response. Moreover, consistent with these findings and our *in vitro* studies, cleaved caspase 3 staining, a marker of apoptosis, was markedly increased following the combination treatment at the 2-week time point (Fig. 4B). No toxicity was observed in tumor-bearing mice even 3 weeks after treatment suspension. Collectively, our *in vivo* data suggest that nongenotoxic p53 reactivation converts a cytostatic activity of temsirolimus into an apoptosis-inducing regiment with high activity in our preclinical models.

Combination of MDM2 and mTORC1 inhibition causes only moderate and transient human myelotoxicity

RG7388 is currently being tested in adults, both alone and in combination with intermittent schedules, which allows a faster bone marrow recovery, showing favorable responses in highly pretreated patients. Because MDM2 inhibitors have predominantly caused myelotoxicity in clinical trials, we evaluated the effect of the combination RG7388 and temsirolimus on both human PBMCs viability and CFU generation of human $CD34^+$ HSPCs. Doses of RG7388 and temsirolimus that showed *in vitro* antitumor activity did not affect cell viability, apoptosis, and subpopulations' distribution of PBMCs from three separate donors (Supplementary Figs. S5 and S6). Moreover, 14-day treatment with RG7388

alone and in combination with temsirolimus did not significantly alter CFU generation of human $CD34^+$ HSPCs from three independent donors. Only a modest decrease in $CD34^+$ CFU was detected with the highest RG7388 concentration (Supplementary Fig. S7). To then address the concern that MDM2 inhibitors have on-target toxicity in humans that has not been seen in rodent models due to limited p53 activation, we developed an *in vivo* system to test the effect of our combination therapy on human lymphocyte reconstitution. Humanized NOD/SCID/IL2rγnull (NSG) mice with greater than 40% human $CD45^+$ reconstitution were treated with vehicle or the combination therapy for 2 weeks, and human and mouse $CD45^+$ cells were evaluated in the peripheral blood at different time points after treatment (Fig. 5A). Percentages of human $CD45^+$ cells significantly drop at day 21 after treatment in mice treated with the combined therapy compared with controls; however, their levels are robustly restored at day 35 after treatment, suggesting only a transient effect of our combined therapy on human lymphocyte reconstitution (Fig. 5B–D).

Combination of MDM2 and mTORC1 inhibition uniquely suppresses survivin sensitizing neuroblastoma cells to apoptosis

To gain insight into the mechanisms underlying the ability of our combination to promote high levels of apoptosis, we looked at changes in expression of different known pro- and antiapoptotic proteins in response to single and combined treatments. As expected, we confirmed the ability of single-agent RG7388 to induce p53 and Bax protein expressions, and the ability of single-agent temsirolimus to repress pS6 levels. However, we did not observe any changes in Bcl2, PUMA, BID, and p73 protein levels following our combination compared with single-agent treatment (Supplementary Fig. S8).

Survivin (BIRC5) levels predict neuroblastoma poor survival and are linked to acquired drug resistance (37). Interestingly, we found that our combination therapy uniquely represses survivin protein levels in all the cell lines tested. This finding was confirmed using both first-generation (Nutlin 3a) and second-generation (RG7388) MDM2 inhibitors (Fig. 6A, C, and D; Supplementary Fig. S9). Moreover, we show that our combination profoundly represses survivin expression at both mRNA and protein levels in wild-type p53 cells (Fig. 6B, 6C, and 6D). However, this effect was totally abrogated when the combination therapy was tested in a p53-mutant line, confirming that a functional p53 is required for survivin suppression (Fig. 6E). This lack of survivin suppression in p53-mutant cells is consistent with the observation that our combination did not induce apoptosis in these cells (Supplementary Fig. S3C). Furthermore, the dual therapy uniquely suppresses RG7388-mediated p21 induction (38), suggesting an additional potential mechanism for the enhanced sensitization (Fig. 6A). We then engineered IMR32 cells to express high levels of survivin (Fig. 7A) and asked whether we could rescue the effect of the combination therapy on cell apoptosis. Although conditional overexpression of survivin did not affect temsirolimus-mediated apoptosis, and only moderately attenuated Nutlin 3a-mediated apoptosis, it profoundly impaired the apoptosis induced by the combination therapy (P =0.030; Fig. 7B), suggesting that the suppression of survivin contributes to the efficacy of our combination therapy. In addition, pharmacologic inhibition of survivin via YM155 significantly enhances the apoptosis induced by the combination therapy (P = 0.017), confirming the protective role of survivin (Fig. 7C).

Discussion

Enhanced protein synthesis by MYCN is critical for its oncogenic functions (6). Thus, mTOR blockade by inducing MYCN destabilization represents an effective way of targeting this MYCN function (39). Although well tolerated, temsirolimus showed modest activity as single agent in a phase II study in children with solid tumors (19). Diverse adaptive processes have been linked to acquired resistance to mTORC1 inhibitors, including upregulation of glutamine metabolism, PTEN expression, and negative feedback activation of PI3K/AKT signaling (40, 41). Therefore, we sought to identify ways to improve the clinical activity of mTORC1 inhibitors for MYC-driven tumors via rational drug combination. Supporting this concept, combinations of mTORC1 inhibitors with other treatment modalities (*e.g.,* cytotoxic chemotherapy, hormonal therapy, and targeted agents) have shown promising results in different tumor models (42, 43). We present here a novel potent combination for neuroblastoma therapy by adding non-genotoxic p53 reactivation to mTORC1 inhibition.

Although it is known that p53 inhibits mTORC1 in response to cellular stress, the complexity of the interplay between p53 and mTOR has been only partially explored and is context-dependent. Activated p53 inhibits mTORC1 through AMPK and REDD1 via TSC1/2 complexes (44). Conversely, mTOR signaling positively regulates p53 function under certain circumstances (45). Our data confirm that p53 effectively suppresses mTOR signaling in neuroblastoma by inducing negative regulators of the PI3K/AKT/mTOR pathway. They also indicate that p53 is one of the factors that potentially affect the response to mTORC1 inhibition.

Importantly, our *in vivo* data suggest that dual inhibition of MDM2 and mTOR signaling is highly effective in blocking neuroblastoma tumor growth. Supporting our findings, it has been shown that inhibition of mTOR signaling sensitizes p53 wild-type neuroblastoma cells to genotoxic-induced apoptosis (46). In our neuroblastoma models, single-agent temsirolimus does not induce apoptosis both in cells and xenografts, and tumors rapidly regrow after therapy withdrawal. However, *in vivo* dual inhibition of MDM2 (via RG7388) and mTOR signaling dramatically blocks neuroblastoma tumor growth and most importantly results in a sustained antitumor response due to p53-mediated induction of apoptosis.

Second-generation MDM2 inhibitors have been recently developed. A phase I trial with the first molecule RG7112 demonstrated clinical activity in patients with leukemias (47). However, the dose required for efficacy led to neutropenia, thrombocytopenia, and GI intolerance (47). MDM2 is critical for normal hematopoiesis, and treatment with MDM2 antagonists leads to bone marrow suppression of normal progenitors. To address this issue, RG7388 (Idasanutlin), a second-generation MDM2 inhibitor from Hoffman-La Roche with enhanced potency, selectivity, and bioavailability, has been recently developed and formulated for oral administration. RG7388 is currently being tested in adult patients with solid and hematologic malignancies, both as single agent and in combination with conventional and targeted therapies (e.g., NCT02633059, NCT02828930, and NCT02545283). This study evaluates for the first time the effect of RG7388 in combination with temsirolimus on neuroblastoma tumor growth, providing valuable preclinical data that

will guide future clinical efforts in pediatrics. The development of more selective and potent compounds (such as RG7388), together with the identification of effective combinations (such as RG7388 and temsirolimus), will allow to achieve higher clinical efficacy with lower toxicity. This is supported by our *in vivo* studies, which demonstrated only a transient suppression of human $CD45^+$cells following the treatment with our combination.

Biochemical analyses of neuroblastoma cells also indicate that a potential mechanism underlying the efficacy of our combination is the p53-mediated suppression of survivin. Survivin is overexpressed in neuroblastoma, and its expression strongly correlates with patient poor survival (48). Differential expression of survivin in tumors is transcriptionally regulated by oncogenic signaling (e.g., IGF-1/mTOR signaling; ref. 49) and loss of p53-mediated gene repression (50). Our data show that the combination therapy uniquely suppresses survivin protein levels in a p53-dependent manner, promoting cell death. In turn, ectopic expression of survivin confers resistance to the combination therapy. This observation suggests that nongenotoxic p53 activation enhances temsirolimus activity via p53-dependent inhibition of survivin and supports a role for survivin in chemoresistance and tumor relapse. Of note, therapeutic targeting of survivin is currently under investigation with great potential (51). However, another possible mechanism of action for our combination is the suppression of p53-mediated upregulation of p21 (CDKN1A). p21 is a critical cell-cycle regulator, which may counteract induction of apoptosis.

Increasing evidence shows that the PI3K/Akt/mTOR pathway plays an important role in the development and progression of neuroblastoma. Our *in vivo* studies clearly demonstrate that nongenotoxic p53 activation via RG7388 strongly enhances the antitumor activity of temsirolimus, leading to improved efficacy and limited toxicity. This combination warrants testing in early-phase clinical trials.

Acknowledgments

We thank members of the Roche Pediatric MDM2 Antagonist Consortium for their helpful contributions: Steve Middleton, Gwen Nichols, and Raphaël Rousseau.

Grant Support

This study was supported by the Children's Cancer Research Fund (E. Barbieri), the St. Baldrick's Foundation (E. Barbieri), and Hyundai Hope on Wheels (E. Barbieri).

References

1. Maris JM. Recent advances in neuroblastoma. N Engl J Med. 2010; 362:2202–11. [PubMed: 20558371]
2. Carr-Wilkinson J, O'Toole K, Wood KM, Challen CC, Baker AG, Board JR, et al. High frequency of p53/MDM2/p14ARF pathway abnormalities in relapsed neuroblastoma. Clin Cancer Res. 2010; 16:1108–18. [PubMed: 20145180]
3. Zirath H, Frenzel A, Oliynyk G, Segerstrom L, Westermark UK, Larsson K, et al. MYC inhibition induces metabolic changes leading to accumulation of lipid droplets in tumor cells. Proc Natl Acad Sci U S A. 2013; 110:10258–63. [PubMed: 23733953]
4. Westermark UK, Wilhelm M, Frenzel A, Henriksson MA. The MYCN oncogene and differentiation in neuroblastoma. Semin Cancer Biol. 2011; 21:256–66. [PubMed: 21849159]

5. Chanthery YH, Gustafson WC, Itsara M, Persson A, Hackett CS, Grimmer M, et al. Paracrine signaling through MYCN enhances tumor-vascular interactions in neuroblastoma. Sci Transl Med. 2012; 4:115ra3.
6. Pourdehnad M, Truitt ML, Siddiqi IN, Ducker GS, Shokat KM, Ruggero D. Myc and mTOR converge on a common node in protein synthesis control that confers synthetic lethality in Myc-driven cancers. Proc Natl Acad Sci U S A. 2013; 110:11988–93. [PubMed: 23803853]
7. Ravitz MJ, Chen L, Lynch M, Schmidt EV. c-myc Repression of TSC2 contributes to control of translation initiation and Myc-induced transformation. Cancer Res. 2007; 67:11209–17. [PubMed: 18056446]
8. Shaw RJ, Cantley LC. Ras, PI(3)K and mTOR signalling controls tumour cell growth. Nature. 2006; 441:424–30. [PubMed: 16724053]
9. Weber A, Huesken C, Bergmann E, Kiess W, Christiansen NM, Christiansen H. Coexpression of insulin receptor-related receptor and insulin-like growth factor 1 receptor correlates with enhanced apoptosis and dedifferentiation in human neuroblastomas. Clin Cancer Res. 2003; 9:5683–92. [PubMed: 14654552]
10. Ho R, Minturn JE, Hishiki T, Zhao H, Wang Q, Cnaan A, et al. Proliferation of human neuroblastomas mediated by the epidermal growth factor receptor. Cancer Res. 2005; 65:9868–75. [PubMed: 16267010]
11. Matsui T, Sano K, Tsukamoto T, Ito M, Takaishi T, Nakata H, et al. Human neuroblastoma cells express alpha and beta platelet-derived growth factor receptors coupling with neurotrophic and chemotactic signaling. J Clin Invest. 1993; 92:1153–60. [PubMed: 8376577]
12. Opel D, Poremba C, Simon T, Debatin KM, Fulda S. Activation of Akt predicts poor outcome in neuroblastoma. Cancer Res. 2007; 67:735–45. [PubMed: 17234785]
13. Chesler L, Schlieve C, Goldenberg DD, Kenney A, Kim G, McMillan A, et al. Inhibition of phosphatidylinositol 3-kinase destabilizes Mycn protein and blocks malignant progression in neuroblastoma. Cancer Res. 2006; 66:8139–46. [PubMed: 16912192]
14. Johnsen JI, Segerstrom L, Orrego A, Elfman L, Henriksson M, Kagedal B, et al. Inhibitors of mammalian target of rapamycin downregulate MYCN protein expression and inhibit neuroblastoma growth in vitro and in vivo. Oncogene. 2008; 27:2910–22. [PubMed: 18026138]
15. Cage TA, Chanthery Y, Chesler L, Grimmer M, Knight Z, Shokat K, et al. Downregulation of MYCN through PI3K inhibition in mouse models of pediatric neural cancer. Front Oncol. 2015; 5:111. [PubMed: 26029667]
16. Schulte JH, Schowe B, Mestdagh P, Kaderali L, Kalaghatgi P, Schlierf S, et al. Accurate prediction of neuroblastoma outcome based on miRNA expression profiles. Int J Cancer. 2010; 127:2374–85. [PubMed: 20473924]
17. Houghton PJ, Morton CL, Tucker C, Payne D, Favours E, Cole C, et al. The pediatric preclinical testing program: description of models and early testing results. Pediatr Blood Cancer. 2007; 49:928–40. [PubMed: 17066459]
18. Spunt SL, Grupp SA, Vik TA, Santana VM, Greenblatt DJ, Clancy J, et al. Phase I study of temsirolimus in pediatric patients with recurrent/refractory solid tumors. J Clin Oncol. 2011; 29:2933–40. [PubMed: 21690471]
19. Geoerger B, Kieran MW, Grupp S, Perek D, Clancy J, Krygowski M, et al. Phase II trial of temsirolimus in children with high-grade glioma, neuroblastoma and rhabdomyosarcoma. Eur J Cancer. 2012; 48:253–62. [PubMed: 22033322]
20. O'Reilly KE, Rojo F, She QB, Solit D, Mills GB, Smith D, et al. mTOR inhibition induces upstream receptor tyrosine kinase signaling and activates Akt. Cancer Res. 2006; 66:1500–8. [PubMed: 16452206]
21. Bagatell R, Norris R, Ingle AM, Ahern C, Voss S, Fox E, et al. Phase 1 trial of temsirolimus in combination with irinotecan and temozolomide in children, adolescents and young adults with relapsed or refractory solid tumors: a Children's Oncology Group Study. Pediatr Blood Cancer. 2014; 61:833–9. [PubMed: 24249672]
22. Morgenstern DA, Marzouki M, Bartels U, Irwin MS, Sholler GL, Gammon J, et al. Phase I study of vinblastine and sirolimus in pediatric patients with recurrent or refractory solid tumors. Pediatr Blood Cancer. 2014; 61:128–33. [PubMed: 23956145]

23. Feng Z, Hu W, de Stanchina E, Teresky AK, Jin S, Lowe S, et al. The regulation of AMPK beta1, TSC2, and PTEN expression by p53: stress, cell and tissue specificity, and the role of these gene products in modulating the IGF-1-AKT-mTOR pathways. Cancer Res. 2007; 67:3043–53. [PubMed: 17409411]
24. Budanov AV, Karin M. p53 target genes sestrin1 and sestrin2 connect genotoxic stress and mTOR signaling. Cell. 2008; 134:451–60. [PubMed: 18692468]
25. Feng Z, Levine AJ. The regulation of energy metabolism and the IGF-1/mTOR pathways by the p53 protein. Trends Cell Biol. 2010; 20:427–34. [PubMed: 20399660]
26. Yee KS, Wilkinson S, James J, Ryan KM, Vousden KH. PUMA- and Bax-induced autophagy contributes to apoptosis. Cell Death Differ. 2009; 16:1135–45. [PubMed: 19300452]
27. Parmigiani A, Nourbakhsh A, Ding B, Wang W, Kim YC, Akopiants K, et al. Sestrins inhibit mTORC1 kinase activation through the GATOR complex. Cell Rep. 2014; 9:1281–91. [PubMed: 25457612]
28. Barbieri E, Mehta P, Chen Z, Zhang L, Slack A, Berg S, et al. MDM2 inhibition sensitizes neuroblastoma to chemotherapy-induced apoptotic cell death. Mol Cancer Ther. 2006; 5:2358–65. [PubMed: 16985070]
29. Barbieri E, De Preter K, Capasso M, Johansson P, Man TK, Chen Z, et al. A p53 drug response signature identifies prognostic genes in high-risk neuroblastoma. PLoS One. 2013; 8:e79843. [PubMed: 24348903]
30. Van Maerken T, Ferdinande L, Taildeman J, Lambertz I, Yigit N, Vercruysse L, et al. Antitumor activity of the selective MDM2 antagonist nutlin-3 against chemoresistant neuroblastoma with wild-type p53. J Natl Cancer Inst. 2009; 101:1562–74. [PubMed: 19903807]
31. Ding Q, Zhang Z, Liu JJ, Jiang N, Zhang J, Ross TM, et al. Discovery of RG7388, a potent and selective p53-MDM2 inhibitor in clinical development. J Med Chem. 2013; 56:5979–83. [PubMed: 23808545]
32. Phelps D, Bondra K, Seum S, Chronowski C, Leasure J, Kurmasheva RT, et al. Inhibition of MDM2 by RG7388 confers hypersensitivity to X-radiation in xenograft models of childhood sarcoma. Pediatr Blood Cancer. 2015; 62:1345–52. [PubMed: 25832557]
33. Chen L, Rousseau RF, Middleton SA, Nichols GL, Newell DR, Lunec J, et al. Pre-clinical evaluation of the MDM2-p53 antagonist RG7388 alone and in combination with chemotherapy in neuroblastoma. Oncotarget. 2015; 6:10207–21. [PubMed: 25844600]
34. Patterson DM, Shohet JM, Kim ES. Preclinical models of pediatric solid tumors (neuroblastoma) and their use in drug discovery. Curr Protoc Pharmacol. 2011; Chapter 14(Unit 14):17.
35. Fibach E, Prus E. Differentiation of human erythroid cells in culture. Curr Protoc Immunol. 2005; Chapter 22(Unit 22F):27.
36. Paust S, Bettini M. Daring to learn from humanized mice. Blood. 2015; 125:3829–31. [PubMed: 26089378]
37. Mita AC, Mita MM, Nawrocki ST, Giles FJ. Survivin: key regulator of mitosis and apoptosis and novel target for cancer therapeutics. Clin Cancer Res. 2008; 14:5000–5. [PubMed: 18698017]
38. Beuvink I, Boulay A, Fumagalli S, Zilbermann F, Ruetz S, O'Reilly T, et al. The mTOR inhibitor RAD001 sensitizes tumor cells to DNA-damaged induced apoptosis through inhibition of p21 translation. Cell. 2005; 120:747–59. [PubMed: 15797377]
39. Gustafson WC, Weiss WA. Myc proteins as therapeutic targets. Oncogene. 2010; 29:1249–59. [PubMed: 20101214]
40. Carracedo A, Pandolfi PP. The PTEN-PI3K pathway: of feedbacks and crosstalks. Oncogene. 2008; 27:5527–41. [PubMed: 18794886]
41. Tanaka K, Sasayama T, Irino Y, Takata K, Nagashima H, et al. Compensatory glutamine metabolism promotes glioblastoma resistance to mTOR inhibitor treatment. J Clin Invest. 2015; 125:1591–602. [PubMed: 25798620]
42. Li Z, Yan S, Attayan N, Ramalingam S, Thiele CJ. Combination of an allosteric Akt Inhibitor MK-2206 with etoposide or rapamycin enhances the antitumor growth effect in neuroblastoma. Clin Cancer Res. 2012; 18:3603–15. [PubMed: 22550167]

43. Moore NF, Azarova AM, Bhatnagar N, Ross KN, Drake LE, Frumm S, et al. Molecular rationale for the use of PI3K/AKT/mTOR pathway inhibitors in combination with crizotinib in ALK-mutated neuroblastoma. Oncotarget. 2014; 5:8737–49. [PubMed: 25228590]
44. Feng Z. p53 regulation of the IGF-1/AKT/mTOR pathways and the endosomal compartment. Cold Spring Harb Perspect Biol. 2010; 2:a001057. [PubMed: 20182617]
45. Lee CH, Inoki K, Karbowniczek M, Petroulakis E, Sonenberg N, Henske EP, et al. Constitutive mTOR activation in TSC mutants sensitizes cells to energy starvation and genomic damage via p53. EMBO J. 2007; 26:4812–23. [PubMed: 17962806]
46. Westhoff MA, Faham N, Marx D, Nonnenmacher L, Jennewein C, Enzenmuller S, et al. Sequential dosing in chemosensitization: targeting the PI3K/Akt/mTOR pathway in neuroblastoma. PLoS One. 2013; 8:e83128. [PubMed: 24391739]
47. Andreeff M, Kelly KR, Yee K, Assouline S, Strair R, Popplewell L, et al. Results of the phase I trial of RG7112, a small-molecule MDM2 antagonist in leukemia. Clin Cancer Res. 2016; 22:868–76. [PubMed: 26459177]
48. Lamers F, Schild L, Koster J, Versteeg R, Caron HN, Molenaar JJ. Targeted BIRC5 silencing using YM155 causes cell death in neuroblastoma cells with low ABCB1 expression. Eur J Cancer. 2012; 48:763–71. [PubMed: 22088485]
49. Altieri DC. Validating survivin as a cancer therapeutic target. Nat Rev Cancer. 2003; 3:46–54. [PubMed: 12509766]
50. Hoffman WH, Biade S, Zilfou JT, Chen J, Murphy M. Transcriptional repression of the anti-apoptotic survivin gene by wild type p53. J Biol Chem. 2002; 277:3247–57. [PubMed: 11714700]
51. Garg H, Suri P, Gupta JC, Talwar GP, Dubey S. Survivin: a unique target for tumor therapy. Cancer Cell Int. 2016; 16:49. [PubMed: 27340370]

Translational Relevance

Growing preclinical and clinical evidence indicates that targeting mTOR signaling in combination with genotoxic drugs or targeted biologicals is a potential highly effective approach for different tumor types. Here, we describe a novel therapeutic strategy inhibiting mTORC1 signaling in combination with nongenotoxic p53 reactivation, which overcomes limitations of previous single-agent therapies. We demonstrate that nongenotoxic reactivation of functional p53 suppresses mTOR signaling, and when combined with mTORC1 inhibition profoundly and irreversibly blocks neuroblastoma tumor growth. We also describe a novel role for survivin in chemoresistance and tumor relapse that can be applicable to other tumor types retaining a wild-type p53. Overall, we present preclinical data supporting the further clinical evaluation of the combination temsirolimus plus RG7388 in high-risk neuroblastoma and other tumors with intact p53 signaling.

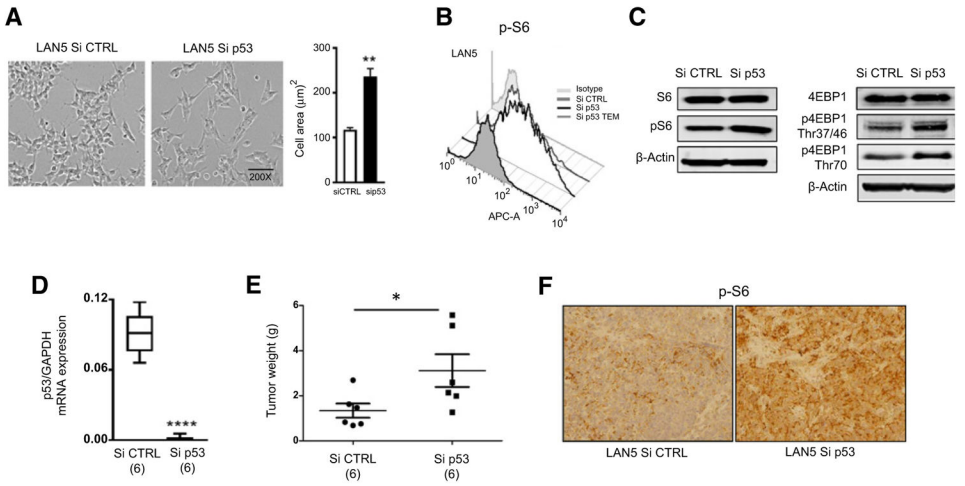

Figure 1.

p53 silencing activates mTOR signaling in neuroblastoma cells and xenografts. **A,** Silencing p53 significantly increases cell size. Cell area from p53-silenced cells was quantitated using ImageJ software; *, $P < 0.05$ by the Student *t* test. **B,** Increased cell size is associated with increased mTOR activity measured as levels of pS6 by flow cytometry. **C,** Western blotting analysis of total S6, pS6, total 4EBP1, and its phosphorylated forms p4EBP1Thr37/46 and p4EBP1Thr70 in Si CTRL and Si p53 LAN5 cells. **D,** Cohorts of 6 mice were orthotopically implanted with Si CTRL and Si p53 LAN5 cells. p53 mRNA expression was confirmed by qPCR in Si CTRL and Si p53 tumors (*t* test, $P = 0.00001$). **E,** Average tumor weights ±SEM (g) of Si CTRL and Si p53 tumors at 3 weeks after implantation. **F,** pS6 levels, analyzed by immunohistochemistry, in Si CTRL and Si p53 tumors. Staining of representative tumors is shown.

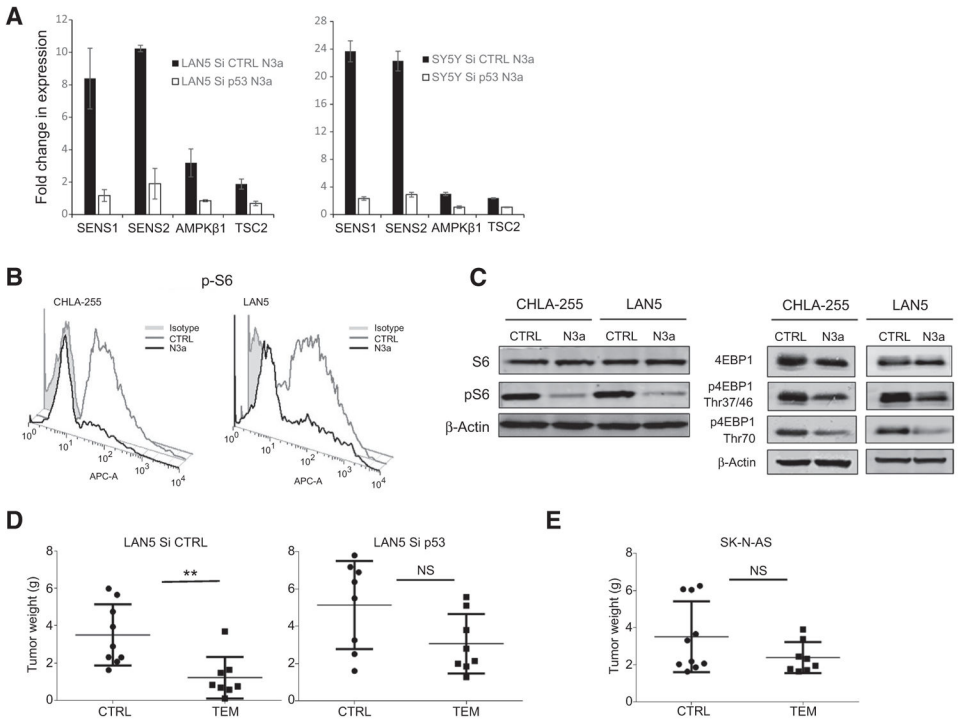

Figure 2.

p53 reactivation inhibits mTOR activity in neuroblastoma cells. **A,** mRNA levels (determined by qPCR) of the mTOR inhibitors SESN1, SESN2, TSC2, and AMPKβ1 in p53 wild-type LAN5 and SH-SY5Y cells upon Nutlin 3a treatment (10 μmol/L for 8 hours). This effect is completely abrogated in LAN5 Si p53 cells. Error bars, two biological replicates. **B,** Nutlin 3a treatment (10 μmol/L for 16 hours) decreases pS6 protein levels as determined by flow cytometry in two p53 wild-type lines (CHLA-255 and LAN5). **C,** Western blotting analysis shows reduced protein levels of both pS6 and p4EBP1 following Nutlin 3a treatment (10 μmol/L for 16 hours) in CHLA-255 and LAN5 cells. p4EBP1 was detected using p4EBP1 Thr37/46 and p4EBP1 Thr70 antibodies, and β-actin served as loading control. **D,** Silencing of p53 attenuates the *in vivo* antitumor effect of temsirolimus (TEM). LAN5 Si CTRL and Si p53 xenografts were generated and treated with either vehicle or temsirolimus (10 mg/kg i.p.) for 2 weeks. Tumor weights at the end of treatment are shown (LAN5 Si CTRL: $P = 0.025$, $n = 9$ in each group; LAN5 Si p53: $P = 0.083$, $n = 8$ in each group). **E,** No significant inhibition of tumor growth by temsirolimus in p53-mutant (SK-N-AS) xenografts ($P = 0.31$, $n = 10$ control and $n = 8$ treated).

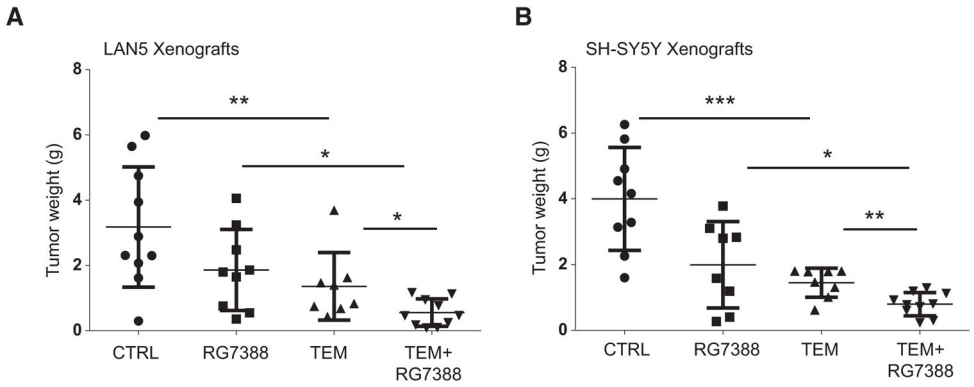

Figure 3.

The combination temsirolimus and RG7388 strongly inhibits neuroblastoma tumor growth. **A,** LAN5 MYCN-amplified xenografts were treated with vehicle, single-agent temsirolimus (10 mg/kg), single agent RG7388 (25 mg/kg), and their combination. Average tumor weights for each cohort ± SEM are shown (n = 10 in each group). Tumors treated with dual therapy are significantly smaller than those treated with single therapy. **B,** SH-SY5Y MYCN nonamplified xenografts received treatment as described above (**A**; n = 10 in each group). Tumors treated with dual therapy are significantly smaller than those treated with single therapies.

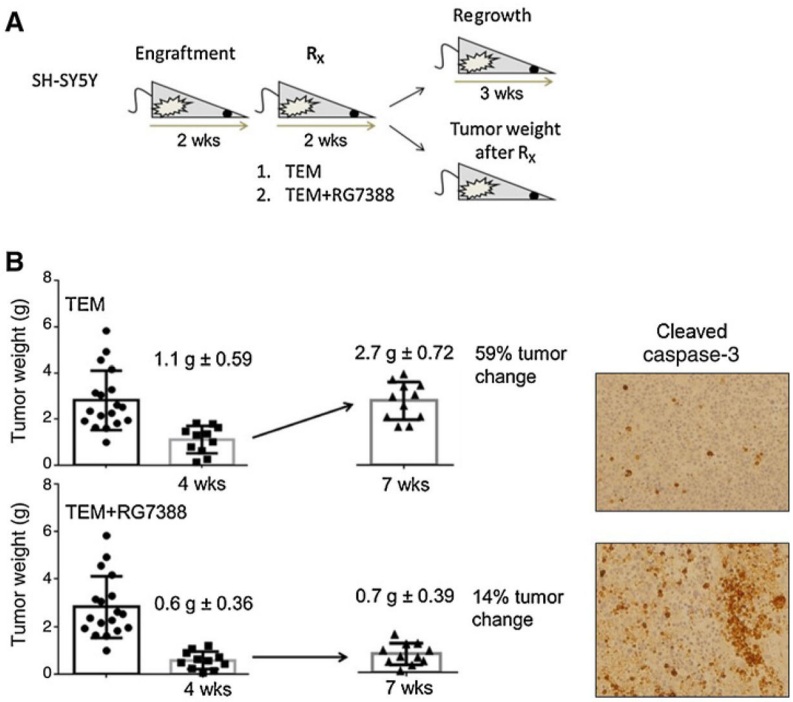

Figure 4.

The combination therapy temsirolimus and RG7388 blocks tumor regrowth after treatment withdrawal. **A,** Schematic representation of the experimental design. SH-SY5Y neuroblastoma cells were orthotopically injected, and three treatment groups of 20 mice each generated: control, temsirolimus (10 mg/kg) as single agent, and temsirolimus in combination with RG7388 (25 mg/kg). After 2 weeks of treatment, half of the mice were sacrificed and tumor weight assessed, and half of the mice kept alive without any additional treatment for 3 weeks. Tumors were followed for 3 weeks after their last treatment. **B,** Average tumor weights for each cohort ± SEM and percentage of tumor change after 2 weeks of treatment and 3 weeks of treatment withdrawal are shown. Single-agent temsirolimus is ineffective in controlling tumor regrowth. However, there is no evidence of tumor regrowth upon dual therapy. Cleaved caspase 3 immunostaining of representative tumor samples from each cohort after 3 weeks of treatment withdrawal is shown.

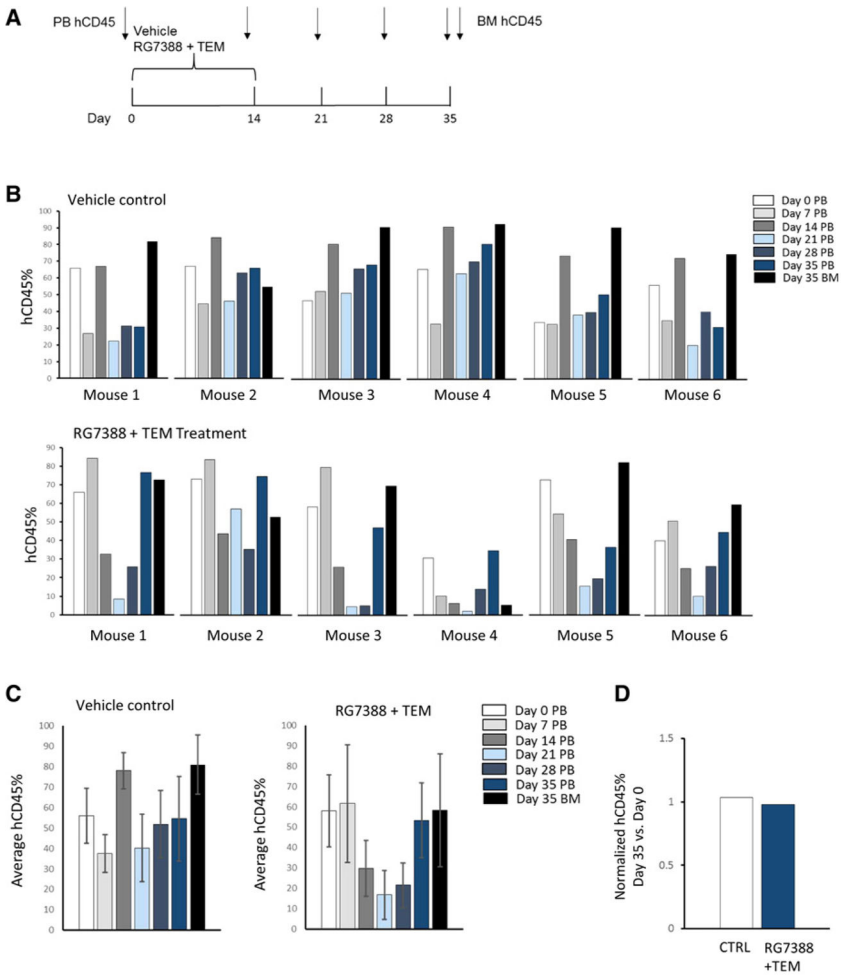

Figure 5.

Effect of the combination RG7388 and temsirolimus on human lymphocyte reconstitution in humanized NSG mice. **A,** Schema of drug treatment and peripheral blood (PB) and bone marrow (BM) collections. **B,** Mice with greater than 40% human $CD45^+$ reconstitution at 7 weeks of age were selected. Six mice received vehicle controls, and six received the combination therapy. Percentages of human $CD45^+$(hCD45) and mouse $CD45^+$(mCD45) cells were assessed in the PB at time 0 and at the indicated time points, and in the BM at day 35 after treatment. Percentages of hCD45 are shown for each individual mouse at the different time points. **C,** Mean values ± SD of hCD45% in control and treated mice at the indicated time points after treatment. Percentages of hCD45 significantly drop at day 21 after treatment in mice treated with the combination therapy compared with controls. However, they are robustly restored at day 35 after treatment. **D,** No differences in percentages of hCD45 in PB were detected at day 35 after treatment between controls and treated mice.

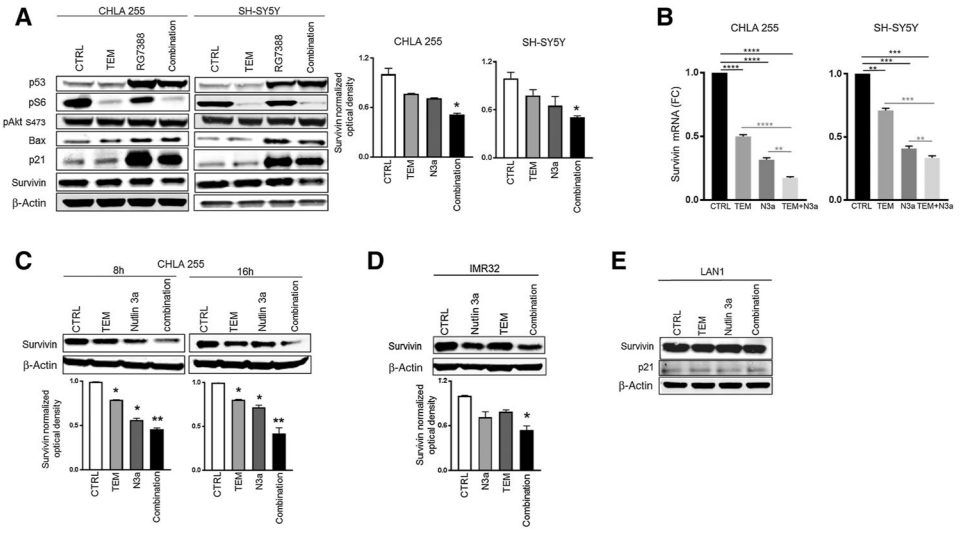

Figure 6.

Dual therapy profoundly downregulates survivin expression. **A,** Expression levels of pro- and antiapoptotic proteins after single and combined treatments in p53 wild-type CHLA255 and SH-SY5Y. Cells were either left untreated (CTRL), treated with 200 nmol/L of RG7388, 5 μmol/L of temsirolimus, or their combination for 16 hours. Protein expression levels were analyzed by Western blotting, and β-actin served as loading control. Western blotting images were quantified by densitometry using Image J Software. Values are mean ±SD of two independent experiments; *, $P < 0.05$ by Student *t* test. **B,** Survivin mRNA expression (determined by qPCR) in CHLA255 and SH-SY5Y cells after single (temsirolimus 10 μmol/L or Nutlin 3a 5 μmol/L) and combined therapy for 16 hours. **, $P < 001$; ***, $P < 0001$; ****, $P < 0.00001$ by Student *t* test; FC, fold change. **C,** Survivin protein expression in CHLA255 cells after single (temsirolimus 10 μmol/L or Nutlin 3a 5 μmol/L) and combined therapy for the indicated time points. **D,** Survivin protein levels in response to single and combined therapy for 16 hours in p53 wild-type IMR32 cells. **E,** Survivin protein levels in p53-mutant LAN1 cells. No changes in expression are detected with both single and combined treatments.

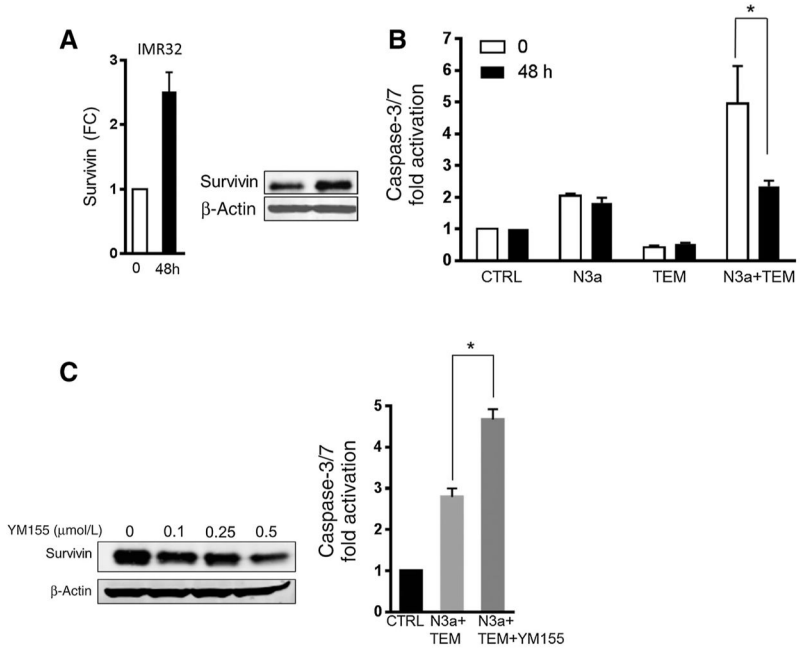

Figure 7.

Survivin overexpression rescues cell apoptosis induced by the dual therapy. **A,** Conditional survivin overexpression was confirmed in IMR32 cells after 48-hour induction with doxycycline by qPCR and Western blotting. **B,** Apoptosis of IMR32 cells with and without survivin overexpression following single and combination therapy for 24 hours. Survivin overexpression significantly attenuates the apoptosis induced by the combination therapy. **C,** Survivin protein levels are suppressed in IMR32 cells following YM155 treatment. Induction of apoptosis in IMR32 cells by the combination therapy with or without YM155 treatment for 24 hours. YM155 significantly potentiates the apoptotic response to the combination therapy.